

# An Analysis of CAN Performance in Active Suspension Control System for Vehicle

Mohd Badril Nor Shah, Abdul Rashid Husain, Amira Sarayati Ahmad Dahalan  
Faculty of Electrical Engineering, Universiti Teknologi Malaysia

**This paper addresses the analysis of control performance for vehicle active suspension via Controller Area Network (CAN) based on full vehicle model. The dynamic model of the system is developed based on four sets of suspension which constitutes 14 state variables communicated through six CAN nodes. The Linear Quadratic Regulator (LQR) technique is used to reduce heave, pitch and roll variation to achieve desired performance of active suspension. The simulation work is performed by using Matlab/Simulink with TrueTime toolbox. Various system performances are analyzed by varying CAN data speed, CAN loss probability, nodes sampling time, clock drift and scheduling techniques. Based on the analysis, the setup of the proposed CAN network for the system meet the system requirements.**

## 1. Introduction

Active suspension is an automotive technology that virtually eliminates heave, pitch and roll variation of onboard systems in many driving situation such as cornering, accelerating, braking and uneven road surface. This technology has always been applied in luxury car, offers a greater degree of ride comfort and car handling. Active suspension consists of spring, viscous damper and actuator, preferably hydraulic actuator, equipped with movement sensors to collect and send amount of information to onboard engine control unit (ECU) to calculate control signal for actuators. Actuators then generate an appropriate force to compensate heave, pitch and roll variation to achieve a great performance of active suspension.

In practical situation, control of active suspension in car is done through network. This constitutes a typical networked control system. All sensors, actuators and controllers are communicated through a shared bus. This type of architecture offer

many advantages, such as reduce complexity of wiring, lower installation cost, enable mobile operation and easy for diagnosis and troubleshooting. However, employing such architecture give arise a new problems, that are time delay and data dropout which can degrade the control performance.

CAN Controller Area Network (CAN) is an advanced serial bus system with high speed, high reliability and low cost for distributed real time control applications. It was initially developed for automotive use in late 1980s by Robert Bosch, but now CAN is widely utilized in most real time automation system due to robustness to electrical interferences, ability to self diagnose and data errors repair, high performances, low cost and suitable for harsh environment. CAN uses carrier sense multiple access protocol with collision detection (CSMA/CD) and arbitration on message priority as its communication protocol to that ensures that a message is successfully transmitted to particular node.

In this work, analysis of CAN performance will be done. In order to achieve this, mathematical model of active suspension is first developed based on full car model as discussed in Section 2. Section 3 deal with the design of Linear Quadratic Regulator (LQR) controller for regulation of active suspension. Section 4 show the simulation results and the discussion of the results are also provided. Finally, Section 5 contains the conclusion.

## 2. Mathematical model of active suspension based full car model

The model of full-vehicle suspension system is adopted from [1], as illustrated in Figure

1. Each set of suspension consists of a spring, a shock absorber and a hydraulic actuator at each corner of the sprung mass (vehicle body). The suspensions connects the sprung mass to the four unsprung masses (front-left, front-right, rear-left and rear-right wheels). This configuration allows sprung mass to heave, pitch and roll freely and enable the unsprung masses are to bounce vertically with respect to the sprung mass. With assumption that all displacements of heave, pitch and roll angles are small, the suspensions between the sprung mass and unsprung masses are modeled as linear viscous dampers while the tires are modeled as simple linear

$$\begin{aligned}
\dot{x}_1 &= x_2 \\
\dot{x}_2 &= -\frac{(2K_{sf}+2K_{sr})}{m_s}x_1 - \frac{(2B_{sf}+2B_{sr})}{m_s}x_2 + \frac{(2aK_{sf}-2bK_{sr})}{m_s}x_3 + \frac{(2aB_{sf}-2bB_{sr})}{m_s}x_4 + \frac{K_{sf}}{m_s}x_7 + \frac{B_{sf}}{m_s}x_8 \\
&\quad + \frac{K_{sr}}{m_s}x_9 + \frac{B_{sr}}{m_s}x_{10} + \frac{K_{sr}}{m_s}x_{11} + \frac{B_{sr}}{m_s}x_{12} + \frac{K_{sr}}{m_s}x_{13} + \frac{B_{sr}}{m_s}x_{14} + \frac{1}{m_s}f_{fl} + \frac{1}{m_s}f_{fr} + \frac{1}{m_s}f_{rl} + \frac{1}{m_s}f_{rr} \\
\dot{x}_3 &= x_4 \\
\dot{x}_4 &= \frac{(2aK_{sf}-2bK_{sr})}{I_{yy}}x_1 + \frac{(2aB_{sf}-2bB_{sr})}{I_{yy}}x_2 - \frac{(2a^2K_{sf}+2bK_{sr})}{I_{yy}}x_3 - \frac{(2a^2B_{sf}+2b^2B_{sr})}{I_{yy}}x_4 - \frac{aB_{sf}}{I_{yy}}x_8 \\
&\quad - \frac{aK_{sf}}{I_{yy}}x_9 - \frac{aB_{sr}}{I_{yy}}x_{10} + \frac{bK_{sf}}{I_{yy}}x_{11} + \frac{bB_{sr}}{I_{yy}}x_{12} + \frac{bK_{sf}}{I_{yy}}x_{13} + \frac{bB_{sr}}{I_{yy}}x_{14} - \frac{a}{I_{yy}}f_{fl} - \frac{a}{I_{yy}}f_{fr} + \frac{b}{I_{yy}}f_{rl} \\
&\quad + \frac{b}{I_{yy}}f_{rr} \\
\dot{x}_5 &= x_6 \\
\dot{x}_6 &= -\frac{w^2(2K_{sf}+2K_{sr})}{4I_{xx}}x_5 - \frac{w^2(2B_{sf}+2B_{sr})}{4I_{xx}}x_6 + \frac{wK_{sf}}{2I_{xx}}x_7 + \frac{wB_{sf}}{2I_{xx}}x_8 - \frac{wK_{sf}}{2I_{xx}}x_9 - \frac{wB_{sr}}{2I_{xx}}x_{10} \\
&\quad + \frac{wK_{sr}}{2I_{xx}}x_{11} + \frac{wB_{sr}}{2I_{xx}}x_{12} - \frac{wK_{sr}}{2I_{xx}}x_{13} - \frac{wB_{sr}}{2I_{xx}}x_{14} + \frac{w}{2I_{xx}}f_{fl} - \frac{w}{2I_{xx}}f_{fr} + \frac{w}{2I_{xx}}f_{rl} - \frac{w}{2I_{xx}}f_{rr} \\
\dot{x}_7 &= x_8 \\
\dot{x}_8 &= \frac{K_{sf}}{m_u}x_1 + \frac{B_{sf}}{m_u}x_2 - \frac{aK_{sf}}{m_u}x_3 - \frac{aB_{sf}}{m_u}x_4 + \frac{wK_{sf}}{2m_u}x_5 + \frac{wB_{sf}}{2m_u}x_6 - \frac{(K_{sf}+K_u)}{m_u}x_7 - \frac{B_{sf}}{m_u}x_8 - \frac{1}{m_u}f_{fl} \\
&\quad + \frac{K_u}{m_u}Z_{r\_fl} \\
\dot{x}_9 &= x_{10} \\
\dot{x}_{10} &= \frac{K_{sf}}{m_u}x_1 + \frac{B_{sf}}{m_u}x_2 - \frac{aK_{sf}}{m_u}x_3 - \frac{aB_{sf}}{m_u}x_4 - \frac{wK_{sf}}{2m_u}x_5 - \frac{wB_{sr}}{2m_u}x_6 - \frac{(K_{sf}+K_u)}{m_u}x_9 - \frac{B_{sf}}{m_u}x_{10} - \frac{1}{m_u}f_{fr} \\
&\quad + \frac{K_u}{m_u}Z_{r\_fl} \\
\dot{x}_{11} &= x_{12} \\
\dot{x}_{12} &= \frac{K_{sr}}{m_u}x_1 + \frac{B_{sr}}{m_u}x_2 + \frac{bK_{sr}}{m_u}x_3 + \frac{bB_{sr}}{m_u}x_4 + \frac{wK_{sr}}{2m_u}x_5 + \frac{wB_{sr}}{2m_u}x_6 - \frac{(K_{sr}+K_u)}{m_u}x_{11} - \frac{B_{sr}}{m_u}x_{12} - \frac{1}{m_u}f_{rl} \\
&\quad + \frac{K_u}{m_u}Z_{r\_rl} \\
\dot{x}_{13} &= x_{14} \\
\dot{x}_{14} &= \frac{K_{sr}}{m_u}x_1 + \frac{B_{sr}}{m_u}x_2 + \frac{bK_{sr}}{m_u}x_3 + \frac{bB_{sr}}{m_u}x_4 - \frac{wK_{sr}}{2m_u}x_5 - \frac{wB_{sr}}{2m_u}x_6 - \frac{(K_{sr}+K_u)}{m_u}x_{13} - \frac{B_{sr}}{m_u}x_{14} - \frac{1}{m_u}f_{rr} \\
&\quad + \frac{K_u}{m_u}Z_{r\_rr}
\end{aligned} \tag{1}$$

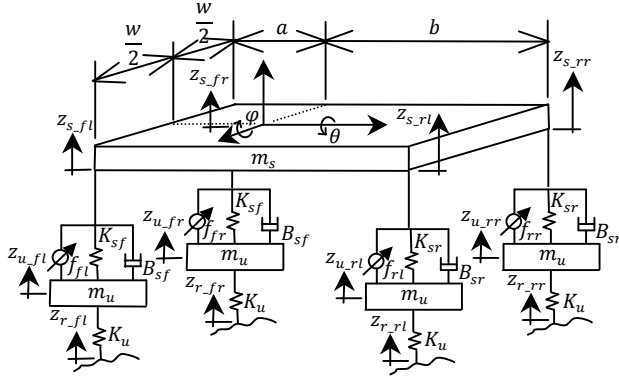


**Figure 1: Active suspension system for full-vehicle model**

springs without damping. Thus, the linearized equation of full-vehicle suspension system is represented as Equation (1).

Equation (1) then is arranged in form of state space equation such that

$$\begin{aligned} \dot{x}(t) &= Ax(t) + Bu(t) + B_d d(t) \\ y(t) &= Cx(t) \end{aligned} \quad (2)$$

where  $y(t)$  is the measured output,  $u(t)$  is force input and  $d(t)$  is disturbance inputs.  $u(t)$  and  $d(t)$  are define as

$$\begin{aligned} u(t) &= [f_{fl}(t) \ f_{fr}(t) \ f_{rl}(t) \ f_{rr}(t)]^T \\ d(t) &= [z_{r-fl}(t) \ z_{r-fr}(t) \ z_{r-rl}(t) \ z_{r-rr}(t)]^T \end{aligned}$$

Note that the subscript 'fl', 'fr', 'rl' and 'rr' are referring to front-left, front-right, rear-left and rear-right of wheels respectively. The state variables  $x(t)$  are assigned as listed in Table 1.

### 3. Controller design

The controller is designed based on continuous optimal state feedback strategy without consider time delay and packet dropout. By considering a state space equation of full-vehicle active suspension system represented in Equation (2), the control input will be in the form of

$$u = -Gx(t) \quad (3)$$

**Table 1: State variables description of active suspension system for full-vehicle model.**

State variables	Description
$x_1 = z$	heave position
$x_2 = \dot{z}$	heave velocity
$x_3 = \theta$	pitch angle
$x_4 = \dot{\theta}$	pitch angular velocity
$x_5 = \varphi$	roll angle
$x_6 = \dot{\varphi}$	roll angular velocity
$x_7 = z_{u,fl}$	front-left wheel unsprung mass height
$x_8 = \dot{z}_{u,fl}$	front-left wheel unsprung mass velocity
$x_9 = z_{u,fr}$	front-right wheel unsprung mass height
$x_{10} = \dot{z}_{u,fr}$	front-right wheel unsprung mass velocity
$x_{11} = z_{u,rl}$	rear-left wheel unsprung mass height
$x_{12} = \dot{z}_{u,rl}$	rear-left wheel unsprung mass velocity
$x_{13} = z_{u,rr}$	rear-right wheel unsprung mass height
$x_{14} = \dot{z}_{u,rr}$	rear-right wheel unsprung mass velocity

where

$$\begin{aligned} u &= [u_1 \ u_2 \ u_3 \ u_4]^T, \\ x(t) &= [x_1 \ x_2 \ x_3 \ \dots \ x_{14}]^T \end{aligned}$$

with  $G$  is an optimal gain which obtained by solving Linear Quadratic Regulation (LQR) problem that minimizes the cost function

$$J = \int_0^{\infty} [x(t)^T Q x(t) + u(t)^T R u(t)] dt \quad (4)$$

where  $Q$  and  $R$  are symmetric positive matrices which penalize the deviation of the state from the origin and the magnitude of the control signal, respectively. The gain  $G$  is given by

$$G = R^{-1} B^T X \quad (5)$$

and  $X = X^T \geq 0$  is the unique positive semi-definite solution of the algebraic Riccati equation

$$A^T X + X A - X B R^{-1} B^T X + Q = 0 \quad (6)$$

The solution of the Riccati equation (6) will lead to the solution of the controller gain  $G$  that takes the system to zero state ( $x(t) = 0$ ) in an optimal controller effort.

However, there in an efficient way emerge recently to solve Equation (6) based on Linear Matrix Inequality (LMI). By the LMI technique, the LQR problem can be rephrased as an optimization problem such that [2]

$$\begin{bmatrix} A^T X + XA + Q & XB \\ B^T X & -R \end{bmatrix} > 0 \quad (7)$$

**4. Simulation results and discussion**

The simulation is done by using Matlab/Simulink with TrueTime toolbox. The parameter of suspension systems are given as shown in Table 2.

For solving the LMI problem of (7), YALMIP/SeDuMi convex problem solver is used instead of using standard LMI toolbox in Matlab. YALMIP/SeDuMi is among the newly developed convex problem solver which is proven to produce a less conservative solution and a higher convergence rate [3]. *Q* and *R* are arbitrarily assigned as

$$Q = \text{diag}(10^8 \ 10^8 \ 10^8 \ 10^8 \ 10^7 \ 10^7 \ 10^7 \ 10^7 \ 10^7 \ 10^7 \ 10^7 \ 10^7)$$

$$R = \text{diag}(0.1 \ 0.1 \ 0.1 \ 0.1)$$

Thus, value of *G* is obtained by using YALMIP/SeDuMi solver such that

$$G = 1 \times 10^4 \begin{bmatrix} 0.2732 & 0.6612 & -0.0554 & \\ 0.4821 & 0.5621 & 0.1733 & \\ 0.0685 & 0.5010 & 0.3095 & \\ 0.0358 & 0.3866 & 0.3950 & \\ -0.3222 & -0.8196 & 0.2871 & 0.5949 \\ -0.3653 & 0.8134 & -0.2819 & -0.2071 \\ 0.2718 & -0.6711 & 0.3123 & -0.9615 \\ 0.1845 & 0.9919 & -0.2785 & -1.7632 \\ -0.1971 & 0.4441 & 0.0131 & 0.2726 \\ 0.0119 & 0.0112 & -0.1922 & -0.3284 \\ -0.0046 & -0.8541 & 0.0001 & 0.8926 \\ 0.0074 & -0.7066 & -0.0047 & -0.1999 \\ -0.0077 & -0.5967 & 0.0086 & \\ 0.0018 & 0.1658 & -0.0071 & \\ -0.1940 & 0.0880 & 0.0270 & \\ 0.0250 & 0.9486 & -0.1921 & \end{bmatrix}$$

To measure the performance of active suspension compare to passive suspension and continuous direct control, integral of

**Table 2: Parameters value of active system suspension system of full-vehicle model [1]**

Descriptions	Value
Sprung mass, <i>m<sub>s</sub></i>	1500 kg
Unsprung mass, <i>m<sub>u</sub></i>	59 kg

Front suspension spring stiffness, <i>K<sub>sf</sub></i>	35000 N/m
Rear suspension spring stiffness, <i>K<sub>sr</sub></i>	38000 N/m
Tire spring stiffness, <i>K<sub>u</sub></i>	190000 N/m
Front suspension damping, <i>B<sub>sf</sub></i>	1000 N/m/s
Rear suspension damping, <i>B<sub>sr</sub></i>	1100 N/m/s
Roll axis moment of inertia, <i>I<sub>xx</sub></i>	460 kg m <sup>2</sup>
Pitch axis moment of inertia, <i>I<sub>yy</sub></i>	2160 kg m <sup>2</sup>
Length between front of vehicle and center of gravity of sprung mass, <i>a</i>	1.4 m
Length between rear of vehicle and center of gravity of sprung mass, <i>b</i>	1.7 m
Width of sprung mass, <i>w</i>	3 m

square of error (ISE) function is used, which defined as

$$ISE = \int_0^\infty [r(t) - c(t)]^2 dt \quad (8)$$

where *r(t)* is set point and *c(t)* is the output parameters that need to measure their performance. In this case, *r(t)* = 0, while heave displacement, pitch angle and roll angle are chosen to evaluate the controlled active suspension performance which is define in (8).

The system is simulated by inserting road disturbance function at the front-right suspension set. The road disturbance *d(t)* will be in form of

$$d(t) = \begin{cases} 0.05(1 - \cos(8\pi t)) & \text{if } 0.5 \leq t \leq 0.75 \\ 0 & \text{otherwise} \end{cases} \quad (9)$$

Four nodes are used to collect necessary information from each four sets of suspension and also responsible to send control signal to actuator of corresponding suspension set. While the other node is used to read sensors for heave, pitch, roll and their derivatives values. All these nodes are communicating with an ECU which calculate a control signal of LQR and send it back to corresponding nodes. The configuration of the nodes is shown in Figure 2 and the tasks details at each node is shown in Table 3.

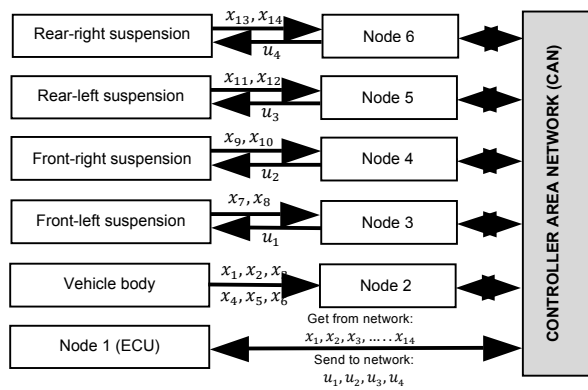


**Figure 2: Nodes configuration of networked control system for full-vehicle model active suspension system**

The system is evaluated in several cases as the following and the results are shown in Table 4 and Figure 3 to Figure 10:

**Case 1:** Sensors sampling time = 0.006s, Controller sampling time = 0.01s, message length = 80 bits, CAN bandwidth = 1Mbps, deploying Dateline Monotonic (DM) scheduling technique for each nodes, no data loss in CAN.

**Case 2:** Sensors sampling time = 0.006s, Controller sampling time = 0.01s, message length = 80 bits CAN bandwidth = 200kbps, deploying DM scheduling technique for each nodes, no data loss in CAN.

**Case 3:** Sensors sampling time = 0.02s, Controller sampling time = 0.01s, message length = 80 bits CAN bandwidth = 1Mbps, deploying DM scheduling technique for each nodes, no data loss in CAN.

**Case 4:** Sensor sampling time = 0.002s, Controller sampling time = 0.01s, message length = 80 bits CAN bandwidth = 1Mbps, deploying DM scheduling technique for each nodes, no data loss in CAN.

**Case 5:** Sensor sampling time = 0.006s, Controller sampling time = 0.01s, message length = 80 bits CAN bandwidth = 1Mbps, deploying DM scheduling technique for each nodes, no data loss in CAN, network always

be interrupt by nodes that contain high priority and random tasks.

**Case 6:** Sensor sampling time = 0.006s, Controller sampling time = 0.01s, message length = 80 bits CAN bandwidth = 1Mbps, DM scheduling technique for each nodes, CAN data loss probability = 0.55.

**Case 7:** Sensor sampling time = 0.006s, Controller sampling time = 0.01s, message length = 80 bits CAN bandwidth = 1Mbps, added with three new task at all nodes with 0.05s execution time each and period time 0.1s, 0.5s and 1s respectively, deploying Earliest Deadline First (EDF) scheduling technique at all nodes, no data loss in CAN.

**Case 8:** Sensor sampling time = 0.006s, Controller sampling time = 0.01s, message length = 80 bits, CAN bandwidth = 1Mbps, DM scheduling technique for each nodes, no data loss in CAN, Node 3 experience clock drift at rate 0.01 (local time drifting 1% faster than nominal time).

The effect of active suspension control performance via CAN with respect to sampling time and CAN data speed are shown in Figure 3 to Figure 6. From the simulation, it is found that the acceptable sensors-controller delay should not be more than 0.05s. Any time delay longer than this value continuously will destabilize the system. In order to obtain good control performance, sampling time and CAN speed must be properly selected. In this case, at sampling time 0.006s and CAN speed 1Mbps, the control performance of LQR for active suspension is almost same with direct control without using network (Figure 3). Increasing sampling time and CAN speed will lead to longer data transmission delay thus degrade the control performance (Figure 4, Figure 5). The delay

**Table 3: Nodes configuration of networked control system for full-vehicle model active suspension system**

Node	Tasks	Task type	Message Priority*	Execution Time (ms)	Period (ms)
1	Received reading for all 14 state variables, calculate control signal of LQR and send it to Node 3, Node 4, Node 5 and Node 6.	Event driven	20,21, 22,23	5	10
2	Get heave displacement sensor reading and send it to Node 1	Clock driven	2	0.9	6
	Get heave velocity sensor reading and send it to Node 1	Clock driven	3	0.9	6
	Get pitch displacement sensor reading and send it to Node 1	Clock driven	4	0.9	6
	Get pitch velocity sensor reading and send it to Node 1	Clock driven	5	0.9	6
	Get roll displacement sensor reading and send it to Node 1	Clock driven	6	0.9	6
	Get roll velocity sensor reading and send it to Node 1	Clock driven	7	0.5	6
3	Get unsprung displacement sensor reading of front-left suspension and send it to Node 1	Clock driven	8	0.9	6
	Get unsprung velocity sensor reading of front-left suspension and send it to Node 1	Clock driven	9	0.9	6
	Receive control signal from Node 1 and send it to actuator of front-left suspension	Event driven	10	0.5	6
4	Get unsprung displacement sensor reading of front-right suspension and send it to Node 1	Clock driven	11	0.9	6
	Get unsprung velocity sensor reading of front-right suspension and send it to Node 1	Clock driven	12	0.9	6
	Receive control signal from Node 1 and send it to actuator of front-right suspension	Event driven	13	0.5	6
5	Get unsprung displacement sensor reading of rear-left suspension and send it to Node 1	Clock driven	14	0.9	6
	Get unsprung velocity sensor reading of rear-left suspension and send it to Node 1	Clock driven	15	0.9	6
	Receive control signal from Node 1 and send it to actuator of rear-left suspension	Event driven	16	0.5	6
6	Get unsprung displacement sensor reading of rear-right suspension and send it to Node 1	Clock driven	17	0.9	6
	Get unsprung velocity sensor reading of rear-right suspension and send it to Node 1	Clock driven	18	0.9	6
	Receive control signal from Node 1 and send it to actuator of rear-right suspension	Event driven	19	0.5	6

\* Priority no.1 is reserved for interference node

**Table 4: Performance comparison of passive suspension and active suspension**

	Heave			Pitch			Roll		
	Passive Suspension	Direct LQR Control	LQR Control via CAN	Passive Suspension	Direct LQR Control	LQR Control via CAN	Passive Suspension	Direct LQR Control	LQR Control via CAN
Case 1	2.627×10 <sup>-4</sup>	5.613×10 <sup>-5</sup>	5.641×10 <sup>-5</sup>	5.512×10 <sup>-5</sup>	1.48×10 <sup>-5</sup>	1.784×10 <sup>-5</sup>	6.648×10 <sup>-4</sup>	2.292×10 <sup>-4</sup>	2.379×10 <sup>-4</sup>
Case 2			3.658×10 <sup>-3</sup>			4.825×10 <sup>-4</sup>			9.802×10 <sup>-3</sup>
Case 3			5.448×10 <sup>-5</sup>			2.778×10 <sup>-5</sup>			3.86×10 <sup>-4</sup>
Case 4			4.85×10 <sup>-5</sup>			4.123×10 <sup>-5</sup>			3.217×10 <sup>-4</sup>
Case 5			2.218×10 <sup>-2</sup>			7.224×10 <sup>-4</sup>			0.122
Case 6			1.508×10 <sup>-4</sup>			7.395×10 <sup>-5</sup>			7.634×10 <sup>-4</sup>
Case 7			6.458×10 <sup>-5</sup>			2.33×10 <sup>-5</sup>			3.521×10 <sup>-4</sup>
Case 8			5.601×10 <sup>-5</sup>			1.742×10 <sup>-5</sup>			2.314×10 <sup>-4</sup>

behavior is random but periodic and bounded at certain range.

Reducing sampling time may fulfill a real time performance, but it might cause a network become saturated and overloaded. Data transmission delay will increase with time, thus destabilizes the active suspension system as shown in Figure 6.

Figure 7 shows the simulation is done by inserting five interference nodes which it injects some high priority and messages at random time into CAN. It is found the delay becomes random and the control performance is significantly degraded.

In CAN, if the data losses occur due to some reason, i.e. error in transmission, or hardware failure, the node will attempt to retransmit the message. This process will increase a delay transmission and become random. Figure 8 shows when the system with loss probability at 55%, sensors-controller delays more than 0.1ms and in random manner. The control performance is significantly degraded and even become unstable if loss probability more than 70%.

Scheduling technique also influence the data transmission delay in a system. In Figure 9, it can be seen that deploying EDF scheduling technique for all nodes will introduce a random and unpredictable sensors-controller delay. However, the control performance is not obviously degraded.

Control performance in a system also can be affected by clock drift phenomenon inside nodes. In Figure 10, it is found the control performance degrade slightly when Node 3 experiences clock drift at rate of 1%. This rate value is chosen since under temperature variation  $-10^{\circ}\text{C}$  to  $50^{\circ}\text{C}$ , drift rate can reach up until 1% due to the sensitivity of quartz clock to temperature [4]. At this rate, sensors-controller delay behavior is random but periodic and at certain period, the delay exceed than 1ms.

From the simulations, the active suspension system using LQR technique is working well under various conditions. With a proper sampling period and CAN data speed, the system preserves the stability when CAN is interrupted by random and high priority tasks, CAN data loss not more than 50% and clock drift at typical rate in particular node.

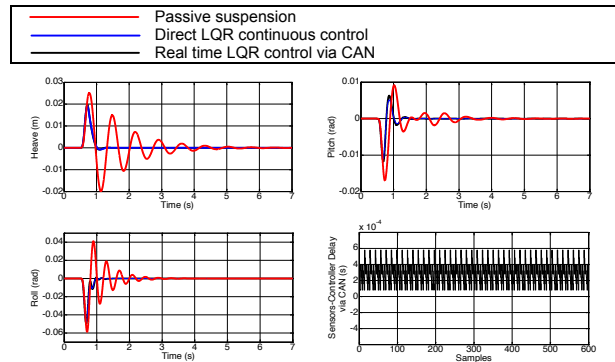


**Figure 3: LQR control performance of active suspension for Case 1**

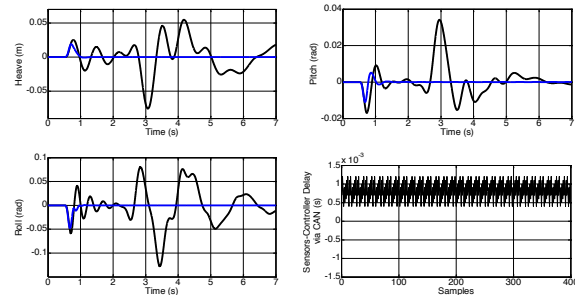


**Figure 4: LQR control performance of active suspension for Case 2**

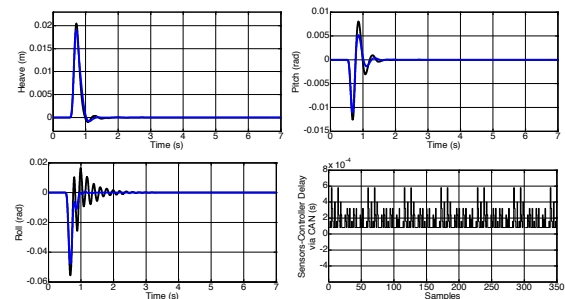


**Figure 5: LQR control performance of active suspension for Case 3**

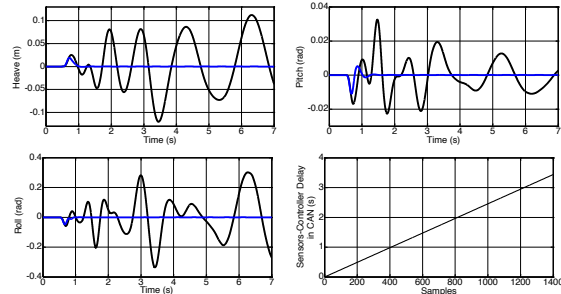


**Figure 6: LQR control performance of active suspension for Case 4**

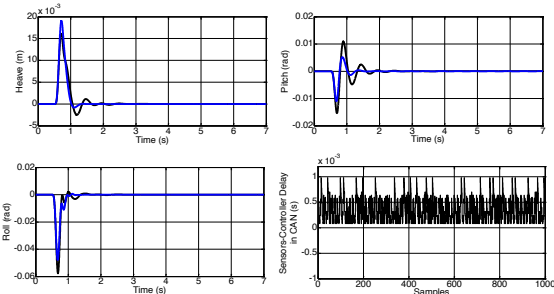


**Figure 7: LQR control performance of active suspension for Case 5**

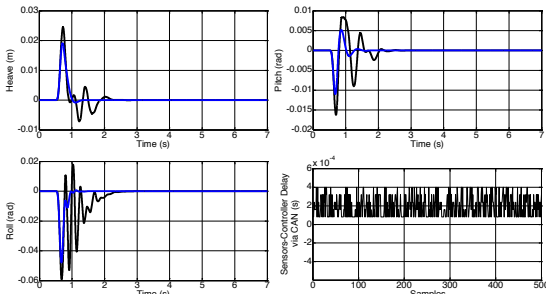


**Figure 8: LQR control performance of active suspension for Case 6**

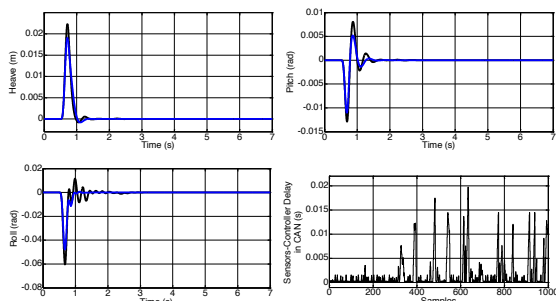


**Figure 9: LQR control performance of active suspension for Case 7**

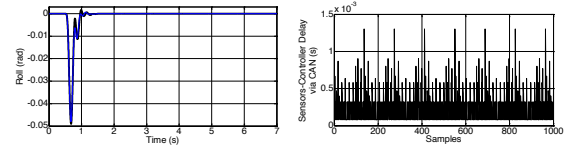
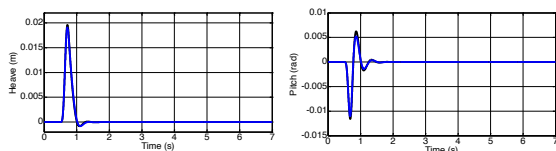


**Figure 10: LQR control performance of active suspension for Case 8**

**5. Conclusion**

The article shows a control of active suspension system using LQR technique. The controller is designed based on continuous system and then be applied into real time system of CAN with help of TrueTime simulator. It is found that the system works well under various conditions and the results also illustrates where the performance of active suspension system is also affected due to variation of CAN system.

**Reference**

- [1] S. Ikenaga, F.L. Lewis, J. Campos, L. Davis, "Active suspension control of ground vehicle based on full-vehicle model", Proceeding of the America Control Conference (ACC), Chicago, USA, 1999.
- [2] Abdul Rashid Husain, "Multi-objective sliding mode control of active magnetic bearing system", PhD thesis, Universiti Teknologi Malaysia, 2009
- [3] J. Lofberg, "YALMIP: A Toolbox for Modeling and Optimization in MATLAB", in Proceeding of the CACSD Conf, Taiwan, 2004. [Online]. Available: <http://control.ee.ethz.ch/~joloef/yalmip.php>
- [4] Aurélien Monot, Nicolas Navet, Bernard Bavoux, "Impact of clock drift on CAN frame response time distribution", Proceedings of IEEE Conference on Emerging Technologies and Factory Automation, 2011

Authors: **Mohd Badril Nor Shah, Abdul Rashid Husain, Amira Sarayati Ahmad Dahalan**

Company: **Universiti Teknologi Malaysia**

Address: **Faculty of Electrical Engineering, 81310 Skudai, Johor Bahru, Malaysia**

Phone: **+607-5535221**

Fax: **+607-5566272**

Email: **bad\_z81@yahoo.com, rashid@fke.utm.my, amira\_sarayati@yahoo.com**

Website: **<http://www.utm.my/fke>**